Molecular Biology of the Cell
Vol. 13, 262–275, January 2002

Actin Dependence of Polarized Receptor Recycling in Madin-Darby Canine Kidney Cell Endosomes[V]

David R. Sheff, Ruth Kroschewski,* and Ira Mellman†

Department of Cell Biology, Ludwig Institute for Cancer Research, Yale University School of Medicine, New Haven, Connecticut 06520-8002

Submitted July 2, 2001; Revised October 1, 2001; Accepted October 26, 2001
Monitoring Editor: David Drubin

Mammalian epithelial cell plasma membrane domains are separated by junctional complexes supported by actin. The extent to which actin acts elsewhere to maintain cell polarity remains poorly understood. Using latrunculin B (Lat B) to depolymerize actin filaments, several basolateral plasma membrane proteins were found to lose their polarized distribution. This loss of polarity did not reflect lateral diffusion through junctional complexes because a low-density lipoprotein receptor mutant lacking a functional endocytosis signal remained basolateral after Lat B treatment. Furthermore, Lat B treatment did not facilitate membrane diffusion across the tight junction as observed with ethylenediaminetetraacetic acid or dimethyl sulfoxide treatment. Detailed analysis of transferrin recycling confirmed Lat B depolarized recycling of transferrin from endosomes to the basolateral surface. Kinetic analysis suggested sorting was compromised at both basolateral early endosomes and perinuclear recycling endosomes. Despite loss of function, these two endosome populations remained distinct from each other and from early endosomes labeled by apically internalized ligand. Furthermore, apical and basolateral early endosomes were functionally distinct populations that directed traffic to a single common recycling endosomal compartment even after Lat B treatment. Thus, filamentous actin may help to guide receptor traffic from endosomes to the basolateral plasma membrane.

INTRODUCTION

Polarized epithelial cells maintain distinct apical and basolateral (BL) plasma membrane domains separated by junctional complexes (Rodriguez-Boulan and Powell, 1992; Drubin and Nelson, 1996; Balda and Matter, 1998). Most membrane proteins are targeted to one domain by distinctive sorting signals (Mellman, 1996). Such sorting events must work in conjunction with cytoskeletal elements such as actin, which also play critical roles in the generation and maintenance of cell polarity. Actin interacts directly or indirectly with a variety of membrane and membrane-associated scaffold components at the tight junction and may also help to establish an intrinsic polarity of cytoskeletal elements throughout the cell (Zahraoui *et al.*, 2000). These interactions may also contribute to establishing a molecular fence between the apical and basolateral domains that prevents the lateral diffusion of membrane proteins and lipids from one domain to the other.

In mammalian epithelial cells, actin may play a role in polarized vesicle transport on the secretory pathway. Myosins I and II have both been associated with *trans*-Golgi network (TGN)-derived transport vesicles (Fath *et al.*, 1997; Stow *et al.*, 1998). Expression of dominant negative Cdc42 (an actin regulatory molecule) in Madin-Darby canine kidney (MDCK) cells misdirects basolateral traffic from the TGN (Kroschewski *et al.*, 1999; Musch *et al.*, 2001). However, it is unknown whether Cdc42 acts in an actin-dependent manner or through some other pathway.

Actin and actin-associated proteins are also involved in the endocytic pathway. Receptor-mediated endocytosis via clathrin-coated pits is restricted to specific sites by the actin cytoskeleton and actin may restrict mobility of newly internalized vesicles (Gaidarov *et al.*, 1999). An increasing number of actin-binding proteins as well as Rho GTPases have also been implicated as being involved in the formation of clathrin-coated vesicles, although it remains unclear whether these elements provide mechanistic or regulatory functions (Jackman *et al.*, 1994; Durrbach *et al.*, 1996; Fujimoto *et al.*, 2000; Kessels *et al.*, 2001)

Actin may help propel endocytic vesicles as they traverse the cytosol. Both myosin-based motility and *Listeria*-like actin comet tails have been associated with endosomal vesicles

Article published online ahead of print. Mol. Biol. Cell 10.1091/mbc.01–07-0320. Article and publication are at www.molbiolcell.org/cgi/doi/10.1091/mbc.01–07-0320.

[V] Online version of this article contains video material for Figure 9. Online version available at www.molbiolcell.org.

* Present address: Institute of Biochemistry, ETH-Zentrum CHN, Universitätsstr. 16, 8092 Zürich, Switzerland.

† Corresponding author. E-mail address: ira.mellman@yale.edu.

(Depina and Langford, 1999; Merrifield *et al.*, 1999; Raposo *et al.*, 1999; Taunton *et al.*, 2000). Rho family GTPases are also associated with endosomes (Sonnichsen *et al.*, 2000). Functionally, brush border myosin I and the unconventional mysosin myr4 have been implicated in endocytic traffic. Expression of dominant negative myosin I partially disrupts the polarized recycling of transferrin at the basolateral surface of Caco-2 cells, whereas myr4 may play a role in traffic between endosomal compartments along the recycling pathway (Durrbach *et al.*, 2000; Huber *et al.*, 2000). A similar effect was observed when the cells were treated with the actin-depolymerizing agent latrunculin A. However, on balance, treatment with actin-depolymerizing agents (latrunculin A, latrunculin B, cytochalasin D) and stabilizing agents (jasplakinolide) have yielded mixed results (Gottlieb *et al.*, 1993; Jackman *et al.*, 1994; Durrbach *et al.*, 1996; Lamaze *et al.*, 1997; Maples *et al.*, 1997).

Although actin is implicated in a number of mechanisms required for epithelial polarity, it remains unclear how these mechanisms interact with proteins already present in a polarized distribution at the plasma membrane. We sought to establish whether the actin cytoskeleton acts primarily at the tight junction, separating apical and basolateral domains; or whether it is important for maintaining polarity of endocytic sorting as suggested for delivery of basolateral components from the TGN.

MATERIALS AND METHODS

Biochemical Reagents

All reagents were purchased from Sigma (St. Louis, MO) unless otherwise noted. Alexa-488-transferrin (Tfn), TR-Tfn, antibody labeling kits, and secondary antibodies were purchased from Molecular Probes (Eugene, OR) ^{125}I was purchased from Amersham Biosciences (Piscataway, NJ). Tfn was radioiodinated using Iodo-Gen (Pierce Chemical, Rockford, IL) to ~5 μCi/μg.

Constructs

Tfn receptor (TfnR), Fc-low density lipoprotein receptor chimera (FcLR), and low-density lipoprotein receptor (LDLR) constructs are as previously described (Matter *et al.*, 1993). TfnR was subcloned into the adenovirus system per manufacturer's directions (Quantum Biotechnologies, Montreal, Quebec, Canada).

Fluorescent Imaging of MDCK Cells

Endosomes were visualized with labeled ligands applied to apical or basolateral surfaces of confluent MDCK monolayers cultured in Transwell inserts.

Receptor Expression. Transfected cells were grown and induced as previously described, except that in double expression studies TfnR was expressed using an adenoviral vector that did not visibly affect morphology (our unpublished results; Sheff *et al.*, 1999).

Surface Localization. Cells were fixed with 3% paraformaldehyde and incubated with either monoclonal antibody C7 (against LDLR ectodomain) or monoclonal antibody 2.4G2 (against FcR ectodomain) applied to both sides of the Transwell membrane. Latrunculin B (Lat B; 0.4 μg/ml) was added for 30 min at 37°C before fixation. For FcLR(5-22) and TfnR surface localization, TR-2.4G2 and Alexa-488-Tfn were applied to both surfaces at 0° for 30 min, rinsed briefly in phosphate-buffered saline (at 0°C), and then fixed as described above.

Transferrin Internalization Studies. MDCK expressing FcLR(5-22) and/or TfnR were cultured on Transwell filters. Cells were incubated in serum-free media 37°C for 30 min to deplete endogenous Tfn. To label RE, TR-Tfn (0.1 mg/ml) was internalized basolaterally at 37°C for 30 min and chased for 30 min. Residual ligand was removed with phosphate-buffered saline pH 2.9. To label early endosome (EE) and recycling endosome (RE), the cells were chilled, allowed to bind fluorescein isothiocyanate-Tfn 1 h on ice (0.1 mg/ml), washed, and warmed to 37°C for 2–3 min. For apical versus basolateral Tfn internalization, Tfn was bound to each side for 1 and the label internalized for 3 min at 37°C. Lat B (0.4 μg/ml) was added for the last 10 min of binding on ice and during internalization.

FcLR and TfnR Double Labeling of Endosomes. Doubly expressing cells were prepared as described above. TR-2.4G2 was applied apically and internalized either for 2 min or for 30 min (to equilibration). Alexa-488-Tfn was applied to the basal surface of the Transwell insert on ice then warmed to 37° for 2 or 2 min. Surfaces were acid washed as described above.

Lipid Labeling Studies. MDCK cells were fed 5 mg/ml C_6-*N*-(7-nitrobenz-2-oxa-1,3-diazol-4-yl) ceramide (C_6-NBD ceramide) (Molecular Probes) in ethanol and diluted 1:200 into DMEM (no fetal calf serum) for 30 min on ice then 30 min at 37°C, and finally chased 1 h at 37°C to allow glycosylation by the Golgi and delivery to the plasma membrane. Apical label was extracted with 1% (w/v) bovine serum albumin (BSA) in DMEM (30 min at 10°C). Cells were treated with 0.4 μg/ml Lat B, 0.1% (v/v) dimethyl sulfoxide (DMSO), or 10 mM EDTA for 30 min at 37°C and imaged live.

All images were obtained on a Zeiss LSM 510 confocal (using Zeiss LSM 510 software on a Dell Pentium II computer) or Zeiss Axioplan M microscope (digital camera; Princeton Instruments, Princeton, NJ) driven by Openlab 2.04 (Improvision, Coventry, England) run on an Apple Macintosh G-4. Images were enhanced and combined using Adobe Photoshop (Adobe Systems, Mountain View, CA).

Quantitation of Receptors and Kinetic Observations of Recycling

Either ^{125}I-Tfn or ^{125}I-C7 was bound to the apical or basolateral surface of Transwell-grown MDCK cells for 1 h on ice. Lat B treatment before binding was 0.4 μg/ml for 30 min at 37°C. Equal amounts of label were applied to untransfected cells to obtain nonspecific binding values. Kinetic observations of Tfn recycling internalization, recycling, and transcytosis were performed essentially as described previously (Sheff *et al.*, 1999).

Modeling of Kinetic Data

Modeling of transferrin recycling was performed as described previously beginning with previously derived values for each rate constant (Sheff *et al.*, 1999). Additionally, internalization and rapid return rates were determined for apically bound transferrin (to be published elsewhere).

Models were based on first order rate constants between compartments as described previously. Variables were defined as follows:

BLB = material bound to basolateral membrane
BEE = basolateral early endosomal compartment
RE = common recycling endosome compartment
BL = basolaterally recycled ligand
A = apically released ligand
AB = apically bound ligand
AEE = apical early endosome
k_1 = rate of transport of ligand from BLB to BEE
k_{-1} = rate of transport of ligand from BEE to BLB

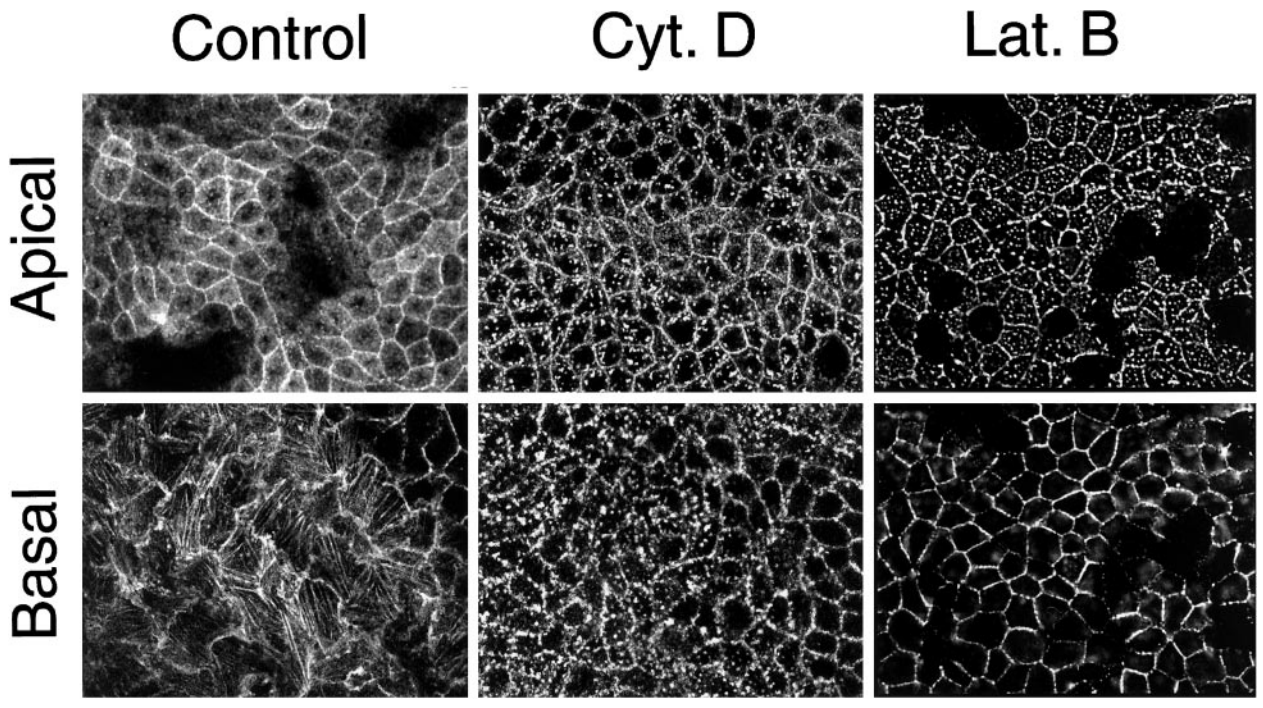

Figure 1. Effects of cytochalasin D and latrunculin of MDCK actin cytoskeleton. Fixed MDCK cells were labeled with Alexa-568 phalloidin after treatment with cytochalisn D (25 μg/ml) or Lat B (0.4 μg/ml). Confocal sections from apical (top row) and basal (bottom row) regions of the cell are shown. Stress fibers are visible in the basal section of untreated cells.

k_2 = rate of transport of ligand from BEE to RE
k_{-2} = rate of transport of ligand from RE to BEE
k_3 = rate of transport of ligand from RE to BL
k_4 = rate of transport of ligand from BEE to BL
k_5 = rate of transport of ligand from RE to A
k_6 = rate of transport of ligand from BEE to A
k_7 = rate of transport of ligand from AB to AEE
k_8 = rate of transport of ligand from AEE to RE
k_{-8} = rate of transport of ligand from RE to AEE
k_9 = rate of transport of ligand from AEE to A
k_{10} = potential rate of transport of ligand from AEE to BL
k_{11} = potential rate of transport of ligand from AEE to BEE
k_{-11} = potential rate of transport of ligand from BEE to AEE

The assignment of rate constants is graphically displayed in Figure 6A. When a pathway is absent, the value k_n is set to zero for that pathway. The equations describing transit of ligand were integrated to yield the following algebraic forms for calculation:

$$BLB = BLB_0\, e^{-k1t} + BEE_0(1 - e^{-k-1t})$$

$$BEE = BEE_0 e^{-(k_{-1}+k_4+k_2+k_{11}+k_6)t} + BLB_0(1 - e^{-k1t}) + RE_0(1 - e^{-k-2t}) + AEE_0(1 - e^{-k-11t})$$

$$RE = RE_0\, e^{-(k_3+k_{-2}+k_{-8}+k_5)t} + AEE_0(1 - e^{-k8t}) + BEE_0(1 - e^{-k2t})$$

$$AEE = AEE_0\, e^{-(k_{-11}+k+k_9+k_{10}+k_{-7})t} + RE^*(1 - e^{-k-8t}) + BEE_0(1 - e^{-k11t}) + AB_0(1 - e^{-k7t})$$

$$AB = AB_0 e^{-k7t} + AEE_0(1 - e^{-k-7t})$$

$$A = A_0 + RE_0(1 - e^{-k5t}) + AEE_0(1 - e^{-k9t}) + BEE_0(1 - e^{-k6t})$$

$$BL = BL_0 + BEE_0(1 - e^{-k4t}) + RE_0(1 - e^{-k3t}) + AEE_0(1 - e^{-k10t})$$

Modeling and curve fitting was performed using Microsoft Excel 98 (Microsoft, Seattle, WA) as described (Sheff *et al.*, 1999) with four separate measurable parameters at each time point (apically and basolaterally released transferrin from cells labeled on the apical or basolateral side). Goodness of fit was determined by sum squared error and statistical comparison of fits was performed by Fischer's F-test as described (Sheff *et al.*, 1999).

RESULTS

Depolymerizing Actin Redistributes Basolateral and Apical Plasma Membrane Markers

The actin cytoskeleton has been implicated in the development of epithelial cell polarity and in particular in the basolateral delivery of nascent proteins (Depina and Langford, 1999; Kroschewski *et al.*, 1999). We therefore sought to examine how actin may be involved in the maintenance of membrane polarity. Lat B is a membrane-permeant actin monomer sequestering drug capable of depolymerizing actin filaments (Spector *et al.*, 1983; Gronewold *et al.*, 1999). Lat B treatment of MDCK cells (0.4 μg/ml) disrupted basolateral actin stress fibers after 10 min with complete dissolution and relocalization of the actin to the lateral margins within 25 min (at 37°C). Subcortical apical actin redistributed to scattered apical dots over the same time course (Figure 1, right column). In contrast, cytochalasin D treatment disrupted basolateral actin stress fibers but created punctate basolateral actin structures (Figure 1, bottom panel, center column) (Maples *et al.*, 1997; Apodaca, 2001). Disruption of

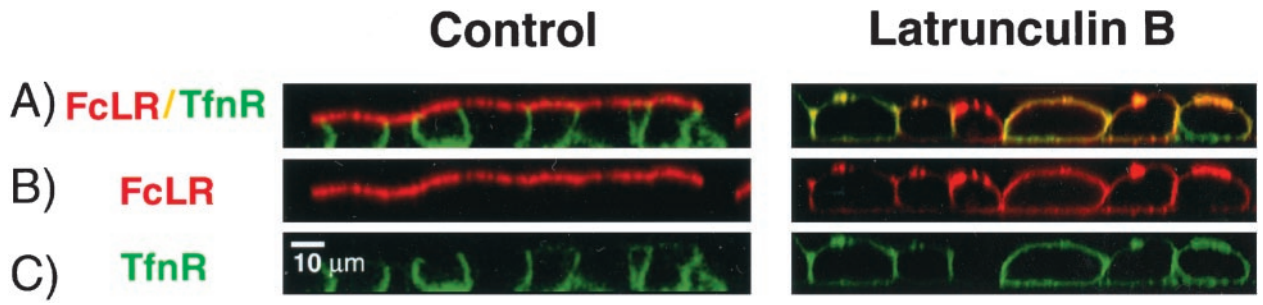

Figure 2. Latrunculin B redistributes polarized receptors in MDCK cells. MDCK cells expressing both the FcR-LDLR chimera [FcLR(5-22)] and human TfnR were grown on Transwell filters. Live cells were labeled with Texas Red-2.4G2 (anti-FcR) and Alexa-488-Tfn from both sides. In control cells, FcLR(5-22) was expressed almost entirely on the apical surface (A and B, left), whereas the TfnR was found at the basolateral surface (A and C, left) After treatment with Lat B (0.4 μg/ml for 30 min), the TfnR redistributed into both the apical and basolateral domains, as does the FcLR (right). Both receptors colocalized along the margins of the basolateral domain as well as in patches in the apical domain (A, right).

apical actin structures was similar for both drugs (Figure 1, top panels).

We examined the effects of Lat B on the polarized distribution of two rapidly internalized plasma membrane receptors. MDCK cells were stably transfected with an apically targeted construct, FcLR(5-22), which consists of the ectodomain of the IgG Fc receptor (FcRBII) fused to the coated pit localization signal of LDLR, eliminating both basolateral targeting sequences but retaining the endocytosis determinant (Matter *et al.*, 1993). In the same cells, a basolaterally targeted wild-type human TfnR was expressed using a recombinant adenovirus.

Untreated cells exhibited a polarized phenotype with the FcLR(5-22) restricted to the apical membrane (Figure 2, A and C, left column) and TfnR restricted to the basolateral membrane as found previously (Figure 2, A and B, left column) (Sheff *et al.*, 1999). Treatment with Lat B for 30 min, however, led to the apparent depolarization of these receptors such that both FcLR and TfnR were now observed in the apical and basolateral regions of almost all cells (Figure 2, right column). No effect was observed at 15 min (our unpublished data).

Latrunculin B Does not Induce Depolarization by Facilitating Lateral Diffusion through Compromised Tight Junctions

Actin is well known to underlie and possibly stabilize junctional complexes. As a result, Lat B might act to disrupt tight junction integrity, resulting in lateral diffusion between apical and basolateral domains. However, Lat B treatment for 30 min did not visibly alter the distribution of the tight junction-associated protein ZO-1 (Figure 3), suggesting that tight junctions remained intact. In contrast, incubation with EDTA (which disrupts cell-cell contacts) for 15 min resulted in the loss of continuous ZO-1 staining at cell margins (Figure 3). DMSO, which disrupts the diffusion barrier to proteins in the axon initial segment by "uncoupling" the plasma membrane from the underlying cytoskeleton (Winckler *et al.*, 1999), had only a slight effect on ZO-1 staining (Figure 3). Nor did DMSO affect TfnR or FcLR(5-22) distribution (our unpublished data).

Lat B treatment may compromise tight junction integrity, however, without obviously affecting ZO-1 staining. To evaluate this possibility, we assayed Lat B-treated monolayers for paracellular leakage. First, we measured transepithelial resistance. An intact monolayer had a resistance of 267 Ohm/cm^2. After Lat B (or DMSO) treatment as described above, this value decreased by ~50% to 140 or 149 Ohm/cm^2, respectively. In contrast, when monolayers were treated with EDTA for just 30 min, transepithelial resistance virtually disappeared (4.5 Ohm/cm^2). Similar results were obtained using trace-labeled ^{125}I-labeled Tfn to measure the leakage of macromolecules from the apical medium. After 30 min, untreated cells leaked 20,000 cpm to the basal medium, Lat B-treated cells 80,000 cpm, and EDTA-treated cells 220,000 cpm. Taken together, these results suggest that tight junction integrity remained relatively intact after Lat B treatment, although there was some loss of function.

To further characterize tight junction activity, we next asked whether Lat B-treated MDCK cells retained a diffusion barrier for lipids by using the fluorescent probe C_6-NBD-ceramide (Lipsky and Pagano, 1983; Van Meer *et al.*, 1987). Label was selectively depleted from the apical surface by extraction with BSA, leaving the basolateral surface selectively labeled with glycosylated NBD lipid. Lat B treatment did not result in any significant apical redistribution of NBD lipids (Figure 4, top). Some of the label was observed in the apical region, although clearly in the subapical cytoplasm because it did not colocalize with apically applied Alexa-594-wheat germ agglutinin (Figure 4, top).

In contrast, treatment with either DMSO or EDTA resulted in redistribution of the NBD-ceramide to the apical plasma membrane in addition to intracellular structures in the apical cytoplasm (Figure 4, bottom). Taken together with the measurements of transepithelial flux, these data suggest that the loss of plasma membrane polarity after Lat B did not result from induced diffusion across a disrupted or compromised tight junction barrier (as in EDTA). If lipids could not pass through tight junctions in Lat B-treated cells, it was highly unlikely that membrane proteins could. Therefore, the ability of Lat B to cause the depolarization of TfnR and LDLR may reflect a pertubation in endocytic membrane traffic. Because bulk lipids such as NBD-ceramide are not

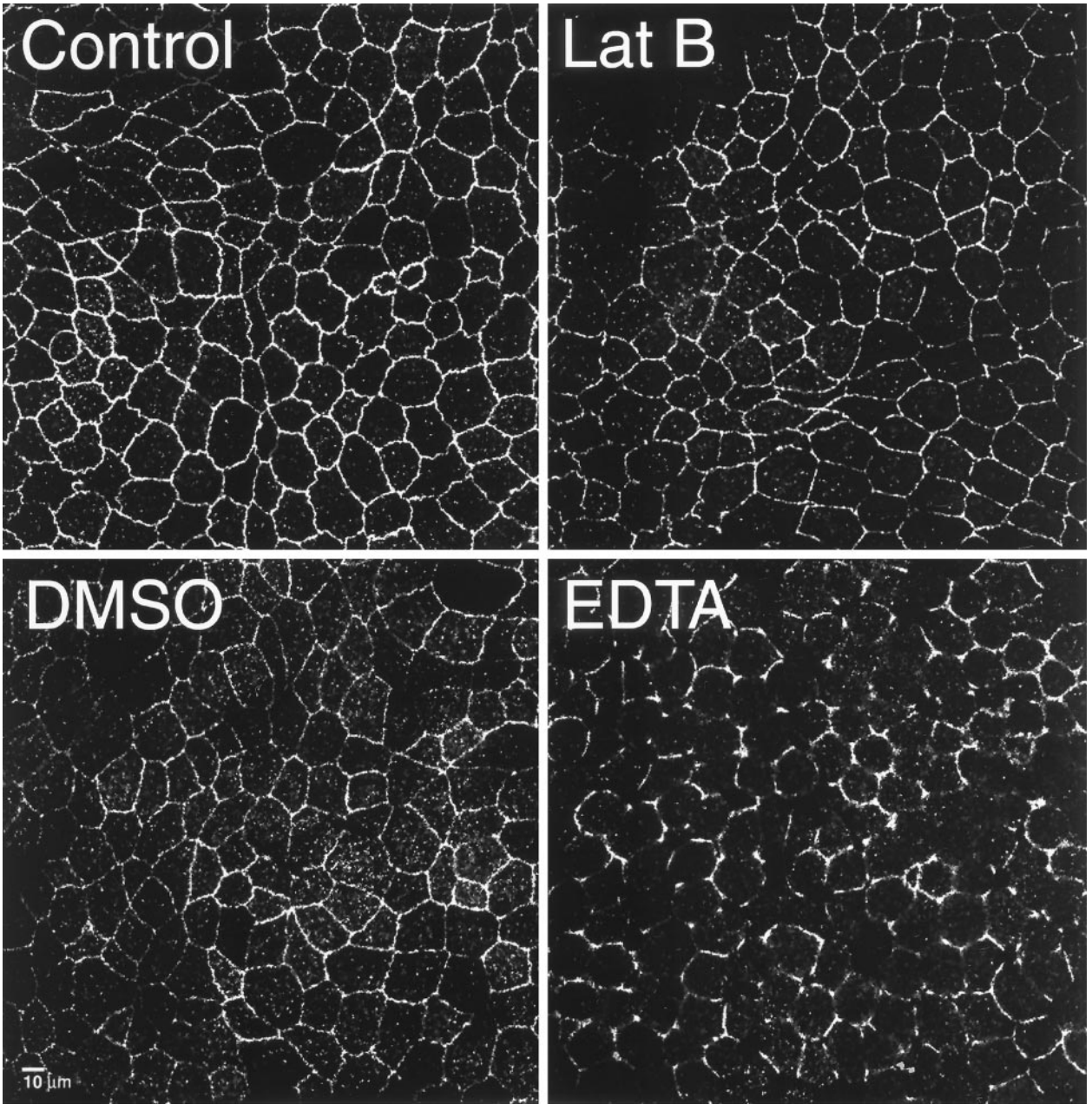

Figure 3. Rapid latrunculin B-induced loss of polarity was not accompanied by a loss of tight junction organization. Confocal optical sections of MDCK monolayers taken of the junctional complex-associated protein ZO-1 at the level of the tight junction in control cells (top left), after treatment with Lat B (top right), DMSO (bottom left), or EDTA (bottom right). All treatments for 30 min at 37°C.

selectively internalized, they may be less susceptible to any such alterations.

Loss of LDL Receptor Polarity Requires Endocytosis

If Lat B disrupted polarity by inhibiting polarized recycling then it should only act on membrane proteins that were capable of rapid endocytosis. We therefore compared redistribution of wild-type LDLR with that of an endocytosis-defective LDLR mutant, 18YA-LDLR (Matter *et al.*, 1993). Both were stably expressed in MDCK cells and found to be restricted to the basolateral domain (Figure 5A, left). After 30 min of Lat B treatment, wild-type LDLR became depolarized in most of the cells (Figure 5A, top right). In sharp contrast, the internalization-defective Y18A LDLR mutant was not redistributed by Lat B treatment, except for a few isolated cells (Figure 5A, bottom right).

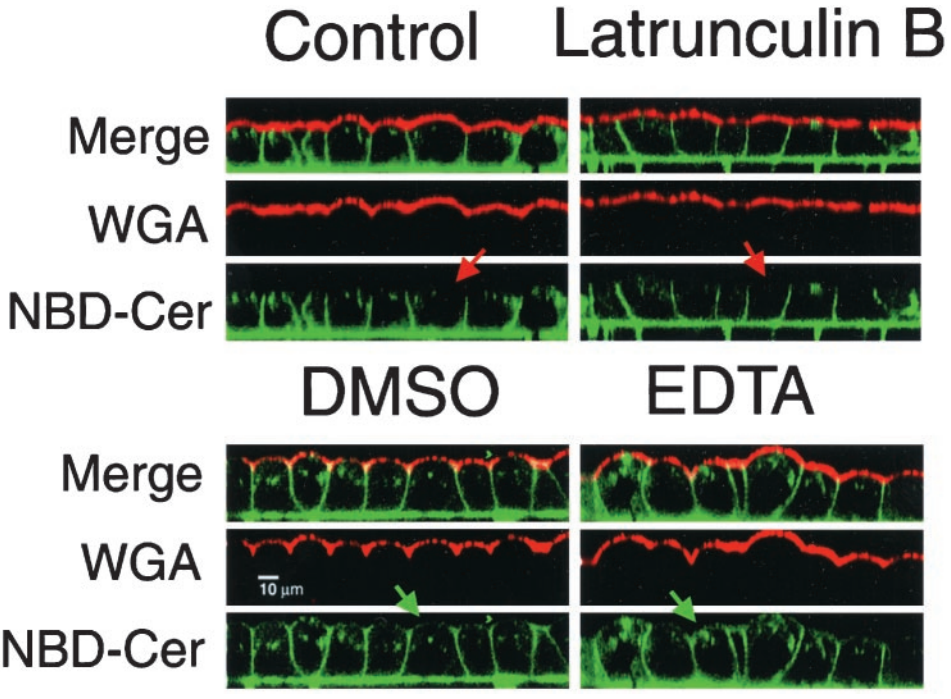

Figure 4. Latrunculin B did not allow free diffusion of lipids across the tight junction. Plasma membrane of MDCK cells labeled with C_6-NBD ceramide (green), which was then depleted from the apical surface with a BSA wash. Cells were then incubated in the presence or absence of various drugs for 30 min. The apical surface was labeled just before imaging with wheat germ agglutinin. In control cells (top left) the NBD-ceramide label was largely basolateral and did not colocalize with the apical marker (red arrow). Lat B treatment (top right) resulted in some redistribution to subapical endosomes and there was flattening of the apical domain, but not colocalization of the basolateral and apical markers (red arrow). In contrast DMSO (bottom left) and EDTA (bottom right) caused movement of lipids across the tight junction from basolateral-to-apical domains (green arrows).

To quantify these results, filter-grown MDCK cells stably transfected with the TfnR, LDLR, or 18YA-LDLR were labeled from the basolateral or apical surfaces with ^{125}I-Tfn or ^{125}I-C7 (an antibody that recognizes the ectodomain of LDLR and 18YA-LDLR). In untreated cells 87% of the surface TfnR was basolateral, as was 85% of LDLR and 86% of 18YA-LDLR (Figure 5B). Lat B treatment for 30 min resulted in a randomization of TfnR distribution (to 50% basolateral) and of the LDLR (to 60% basolateral) but not 18YA-LDLR. Taken together, these results strongly suggest that Lat B-induced redistribution of plasma membrane proteins is dependent upon endocytosis of the protein, and by extension suggest that depolymerization of actin disrupts endosomal sorting or trafficking.

Actin Depolymerization Inhibits Polarized Recycling of Transferrin

The Lat B analog latrunculin A has recently been found to cause ~20% missorting of preinternalized Tfn to the apical side in Caco-2 cells (Durrbach *et al.*, 2000). Because the Caco-2 monolayers were found not to have appreciably lost transepithelial electrical resistance after treatment, it was presumed that apical release of Tfn was due to intracellular missorting. However, it was unclear which endosome population(s) was affected by latrunculin treatment. Stimulated by these results, we next characterized the effects of Lat B on the polarity of Tfn recycling in MDCK cells in greater detail.

To facilitate a kinetic analysis of endocytic trafficking, filter-grown MDCK cells were labeled on the basolateral surface with ^{125}I-Tfn on ice. By starting the experiment with all labeled Tfn at the plasma membrane, it was possible to monitor Tfn through all compartments of the endocytic pathway (Sheff *et al.*, 1999; Brown *et al.*, 2000). After 60 min, 85% of the labeled Tfn was recycled into the basolateral media, 7% was transcytosed (basolateral to apical) into the apical media, and the remainder stayed associated with the cells and filter. Treatment with Lat B (10 min at 0°C and in the chase media) dramatically randomized Tfn recycling (49% basolateral, 45% transcytosed) (Figure 6A). This effect was significantly larger than that observed by Durrbach and colleagues with Lat A (Durrbach *et al.*, 2000) and may reflect the added contribution of missorting from the early endosomes. In contrast, 25 μg/ml cytochalasin D did not alter basolateral Tfn recycling, in agreement with previous observations (Maples *et al.*, 1997; our unpublished data). Lat B sequesters actin monomers and does not compete with actin-capping proteins, thus may be a more effective actin-depolymerizing drug than cytochalasin D (Wakatsuki *et al.*, 2001).

Apical recycling was monitored by binding labeled Tfn to the small fraction of TfnR on the apical surface in the transfected MDCK cells (~15% of the surface total) (Figure 6B). Seventy-one percent were recycled apically (released into the apical media), whereas 22% were transcytosed to the basolateral side. After treatment with Lat B, only 60% was recycled, whereas 34% was transcytosed. The effect of Lat B on apical recycling was thus much less pronounced than on basolateral recycling but still significant.

To confirm that the randomization of basolateral Tfn recycling was not due to paracellular leakage, the effect of Lat B on basolateral recycling was compared with that of EDTA. Treatment with EDTA resulted in only 25% mistargeting to the apical media, far less than that seen with Lat B treatment despite the much larger paracellular leakage (see above), confirming that the mistargeting occurred during intracellular sorting.

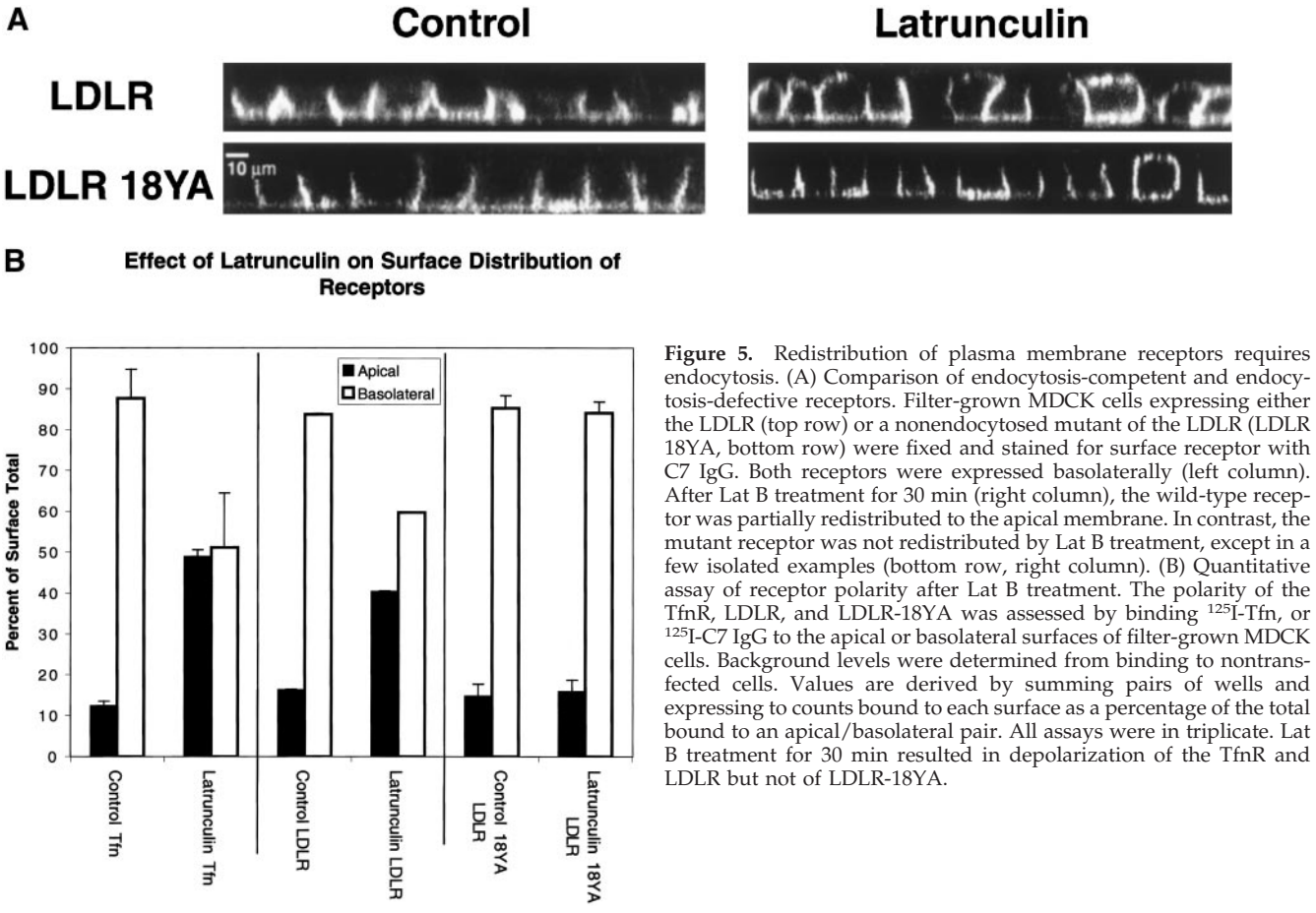

Figure 5. Redistribution of plasma membrane receptors requires endocytosis. (A) Comparison of endocytosis-competent and endocytosis-defective receptors. Filter-grown MDCK cells expressing either the LDLR (top row) or a nonendocytosed mutant of the LDLR (LDLR 18YA, bottom row) were fixed and stained for surface receptor with C7 IgG. Both receptors were expressed basolaterally (left column). After Lat B treatment for 30 min (right column), the wild-type receptor was partially redistributed to the apical membrane. In contrast, the mutant receptor was not redistributed by Lat B treatment, except in a few isolated examples (bottom row, right column). (B) Quantitative assay of receptor polarity after Lat B treatment. The polarity of the TfnR, LDLR, and LDLR-18YA was assessed by binding ^{125}I-Tfn, or ^{125}I-C7 IgG to the apical or basolateral surfaces of filter-grown MDCK cells. Background levels were determined from binding to nontransfected cells. Values are derived by summing pairs of wells and expressing to counts bound to each surface as a percentage of the total bound to an apical/basolateral pair. All assays were in triplicate. Lat B treatment for 30 min resulted in depolarization of the TfnR and LDLR but not of LDLR-18YA.

Polarized Sorting Is Perturbed in Both Early Endosomes and Recycling Endosomes

We next took advantage of our previously characterized system for kinetic analysis of Tfn traffic in MDCK cells to locate steps along the endocytic pathway that might be affected by Lat B (Sheff *et al.*, 1999). This approach uses a total of six separate experimental measurements (clearance from each surface, internalization, and release of Tfn from both the apical and basolateral surfaces) to build a mathematical model of flux through endocytic compartments (Figure 7A). Surface clearance was first calculated from the apical or basolateral surfaces in separate data sets. By using this value, the rapid return rate (k_3 or k_9) was calculated from early time points (<8 min). These values in turn were used in fitting the mathematical construct to data from later time points to derive values for the slower return pathway (e.g., via the RE). Thus, a single modeled set of kinetic values was required to fit data for internalization, recycling, and transcytosis from both surfaces and be valid for both early and late time points. As an additional constraint, the model should predict a 5:1 ratio of IgA to Tfn in the RE when both were basolaterally internalized. This ratio was derived from observations of Brown *et al.* (2000), and in accord with our previously published data for IgA transcytosis (Sheff *et al.*, 1999).

Although a kinetic analysis may not establish a definitive mechanism, it provides an effective and possibly the only means to compare quantitatively intracellular transport steps that do not lend themselves to accurate biochemical determination. We make the assumptions that Tfn is internalized from the basolateral or apical surface first into a compartment of basolateral (or apical) early endosomes. Tfn is then transferred to a single recycling endosome population, or returned rapidly to the basolateral (or apical) plasma membrane. Our previous morphological and cell fractionation analysis of endosomes in MDCK cells provides support for these assumptions, and for the inference that the bulk of internalized Tfn is rapidly recycled back to the basolateral surface without ever reaching the recycling endosome population (Sheff *et al.*, 1999). However, we also considered in the analysis that an additional apical recycling compartment may exist, as suggested by others (Apodaca, 2001).

Internalization rates were directly calculated from the surface clearance data. Rates of transfer between endosomal populations were derived using the internalization rates and

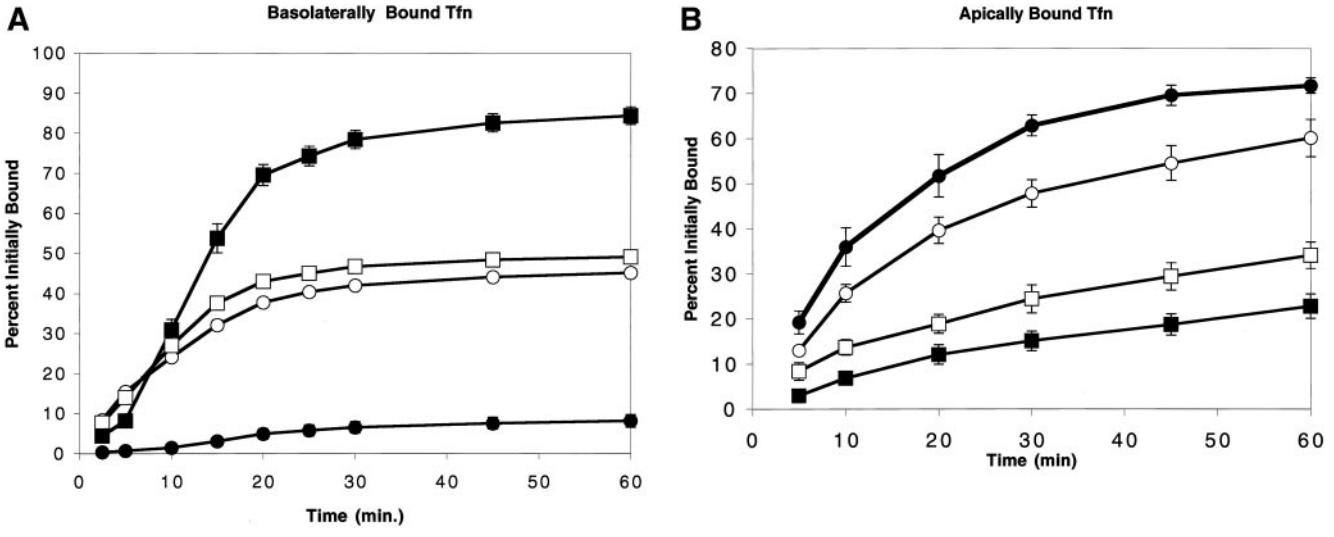

Figure 6. Latrunculin B disrupts endosomal sorting of transferrin. (A) ^{125}I-Tfn bound at 0°C to the basolateral side of MDCK cells was internalized at 37°C and the upper and lower media removed for counting at the intervals shown. In control cells, recycling into the basolateral medium (■) approached 85% after 1 h, with minimal transcytosis to the apical medium (●). Addition of Lat B resulted in randomization of sorting of recycled Tfn to the basolateral (□) and apical (○) media. (B) ^{125}I-Tfn bound to the apical surface recycled largely back to the apical media (●), although apical-to-basolateral transcytosis accounted for up to 25% of the bound Tfn (■). Lat B had a lesser effect on apically internalized Tfn than on the basolaterally endocytosed Tfn. Recycling to the apical side (○) decreased to 60% and apical-to-basolateral transcytosis increased to 35% (□). All values are expressed as a percentage of the total cpm initially bound.

then fitting mathematical curves to the apical and basal release data. The model system is illustrated in Figure 7A (left). Rate equations are as previously published except for the addition of an apical early endosome compartment (Sheff *et al.*, 1999); models using a single early endosome for both apical and basolateral traffic did not fit the data.

We first analyzed endocytosis and recycling of Tfn at the apical surface, because we had not previously analyzed these events. Kinetically, the apical recycling pathway was analogous to its basolateral counterpart. Apical internalization of Tfn to AEE was $k_7 = 0.17$/min, slightly slower than internalization of Tfn from the basolateral surface ($k_1 = 0.21$/min). Rates of return back to the apical surface directly ($k_9 = 0.085$/min) or to a lesser extent via the RE compartment ($k_5 = 0.019$/min) were then calculated (Table 1). Apical recycling differed from basolateral recycling both in the rate of internalization and in that there was significant transcytosis from AEE to the opposite (i.e., basolateral) plasma membrane ($k_{10} = 0.013$). In contrast, BEE to the apical surface traffic was negligible ($k_6 = 0$; Figure 6A).

Surprisingly, Lat B did not affect the rate of surface clearance from either surface (our unpublished data). This differs from published results with the actin-depolymerizing drug cytochalasin D, which demonstrated an inhibition of apical internalization of VSV G protein, although Tfn uptake was unaffected (Gottlieb *et al.*, 1993). These differences may result from measuring Tfn clearance at both the apical and basolateral surfaces in this study or from measuring surface clearance instead of measuring the accumulation of internalized Tfn (Jackman *et al.*, 1994). Using these internalization values, we next derived the rate constants for recycling in Lat B-treated versus untreated cells. As shown in Figure 7C for control cells, the fit of this model to the data (n = 3) was good, with a sum square error (SS) of 103 (where SS = 0 is a perfect fit) and values matched those previously derived (Sheff *et al.*, 1999).

The fit of the control cell model to the Lat B-derived data was not as good (SS = 483), suggesting that Lat B treatment had changed the pathways available for Tfn trafficking (Figure 7C). A better fitting model was obtained by adding a single theoretical pathway (k_6) directly connecting the BEE and the apical plasma membrane (SS = 75). Comparing the basic model (Figure 7A) to this k_6 model (Figure 7A, dashed line) with one degree of freedom difference in the models and 17 degrees of freedom in the k_6 model, Fischer's F-test, F = 92. This indicates that the expanded model fits the Lat B data significantly better ($p < 0.005$) than the basic recycling model (compare Figure 7, D and E). Note the tighter fit of generated curves to data points at earlier times. The greater effect of Lat B on basolaterally versus apically internalized Tfn traffic is reflected in the model by large increase in BEE-to-apical traffic (k_6) but no alteration in traffic from the AEE to the basolateral PM (k_{10}), suggesting a specific effect on the BEE resulting in mistargeting to the apical plasma membrane.

Proposing (mathematically) the existence of unexpected pathways (e.g., direct transport between AEE and BEE, depicted in Figure 7A, left) or the possibility that compartments now thought of distinct are in fact common (e.g., AEE and BEE) does not produce curves that fit the experimental data, either in control or Lat B-treated cells.

Taken together, these results suggest that Lat B may affect traffic from the BEE, possibly allowing transport carriers from this compartment to reach the apical surface without

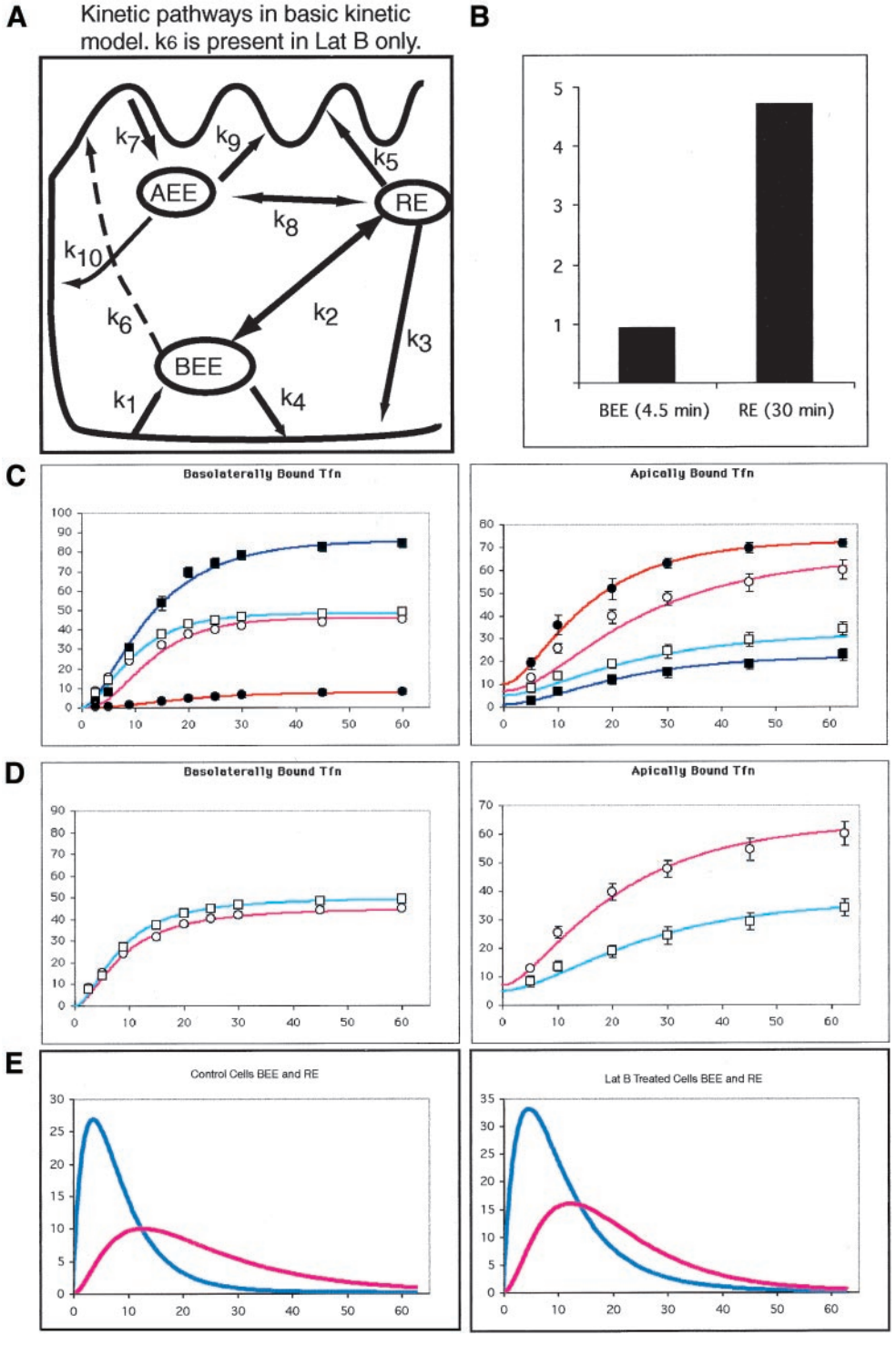

Figure 7. Kinetic modeling of Tfn trafficking and latrunculin B effects. (A) Diagram of possible pathways involved in endocytic traffic from the apical and basolateral surfaces. Kinetic constants are shown for each pathway, values for these constants are given in Table 1. Models including traffic along dashed pathway (k_6) are unique to Lat B-treated cells. (B) Predicted ratio of IgA to Tfn in EE and RE after fitting this model to transcytosis and recycling of apically and basolaterally applied Tfn and basolaterally applied IgA in untreated cells. (C) Left, ^{125}I Tfn was bound to the basolateral then internalized. Counts released into the apical and basolateral media are measured at intervals shown. Data points are the same as in Figure 5. The lines are generated from a mathematical kinetic model. Counts are given as a percentage of the initially bound ^{125}I-Tfn. Control basolateral media data: ■, model: dark blue line. Control apical media data: ●, model: dark red line. Lat B-treated basolateral media data: □, model: light blue line. Lat B-treated apical media data: ○, model: light red line. Right, trafficking of Tfn bound on the apical surface. Data points are the same as in Figure 5. Symbols are the same as in the left panels. (D) Refitting the model to the same data as described above but adding a single extra pathway (k_6) to the model for Lat B-treated cells. Only the Lat B treatment data is shown. (E) Predicted passage of basolaterally applied Tfn through the BEE (blue lines) and RE (red lines) in untreated (left) and Lat B-treated cells (right).

passing through RE. Examination of the rate constants derived from this model (Figure 7D and Table 1) suggest that there is a second effect of Lat B treatment on basolateral recycling traffic in the RE. The value of k_3, traffic from the RE to the BL plasma membrane, was reduced from 0.07 to 0.02 (a 3.5-fold difference). This would have the functional consequence of depolarizing traffic out of the RE, and may be responsible for most of the missorting observed when cells are preloaded with Tfn, under which conditions the Tfn accumulates in REs (Durrbach *et al.*, 2000).

Table 1. Calculated rate constants

Constant	Control	Lat B no k_6	Lat B with k_6
k_1	0.21	0.21	0.21
k_{-1}	0.028	0.028	0.028
k_2	0.092	0.15	0.062
k_{-2}	0.022	0.04	0.013
k_3	0.07	0.03	0.021
k_4	0.12	0.1	0.143
k_5	0.019	0.2	0.028
k_6			0.12
k_7	0.17	0.17	0.17
k_{-7}	0.05	0.05	0.05
k_8	0.02	0.03	0.08
k_{-8}			
k_9	0.085	0.02	0.051
k_{10}	0.013	0.015	0.016
k_{11}			
k_{-11}			
SS	102	483	75

Latrunculin B Treatment Alters Spatial Distribution of MDCK Cell Endosomes

Lat B might stimulate missorting in BEEs by altering their spatial distribution in the cytoplasm or their sorting mechanism. To determine the effect of Lat B on endosome distribution, we first separately labeled BEE and AEE with brief pulses of Tfn internalized simultaneously from the apical and basolateral surfaces (Figure 8A). As has been observed with fluid phase uptake, apical and basolateral Tfn appeared in distinct nonoverlapping EE compartments (Parton *et al.*, 1989; Bomsel *et al.*, 1990). Lat B did not result in a physical merging of these compartments, but did cause the appearance of basolaterally internalized Tfn in more central and apical regions of the cytoplasm (Figure 8B). Thus, the spatial distribution of BEE may be in part controlled by actin.

Next, the BEE and RE were separately labeled with two sequential basolateral pulses of Tfn (Texas Red-Tfn internalized for 30 min followed by Alexa-488-Tfn for 3 min). As demonstrated previously, this regimen resulted in the labeling of BEE and RE in a nonoverlapping distribution (Figure 8C), which was unaffected by Lat B (Figure 8D) (Sheff *et al.*, 1999). Again, some of the BEE could now be observed in the apical cytoplasm.

Finally, the confluence of apical and basolateral endocytic pathways was visualized. The apical pathway was labeled to equilibrium by using a Texas Red-tagged antibody bound to the apically recycling FcLR chimera. The REs were then labeled with Alexa-488-Tfn from the basolateral side as before. Apical and basolateral markers appeared at least in part to colocalize in RE, as reported previously (Hughson and Hopkins, 1990; Odorizzi *et al.*, 1996; Sheff *et al.*, 1999; Leung *et al.*, 2000) (arrowheads, Figures 8D and 9, supplemental reconstruction QuickTime video). After Lat B treatment, however, the extent of colocalization was reduced, although some structures did appear to contain both labels (Figure 8E, arrowheads). This was unexpected and suggests that Lat B restricts the ability of apical and basolateral recycling receptors to enter a common RE population.

DISCUSSION

Actin is clearly involved in endocytic processes. Yeast and mammalian studies alike confirm that even the initial internalization of clathrin-coated vesicles is at least regulated by a family of proteins that interact with or modify the actin cytoskeleton. These include members of the Rho GTPase family, Eps15 family members, and Huntington-interacting type proteins (Ellis and Mellor, 2000; Fujimoto *et al.*, 2000). Actin is also involved in various postendocytic events, including myosin-dependent or actin comet tail-driven vesicle motility (Durrbach *et al.*, 1996; Gaidarov *et al.*, 1999; Merrifield *et al.*, 1999; Raposo *et al.*, 1999; Durrbach *et al.*, 2000;

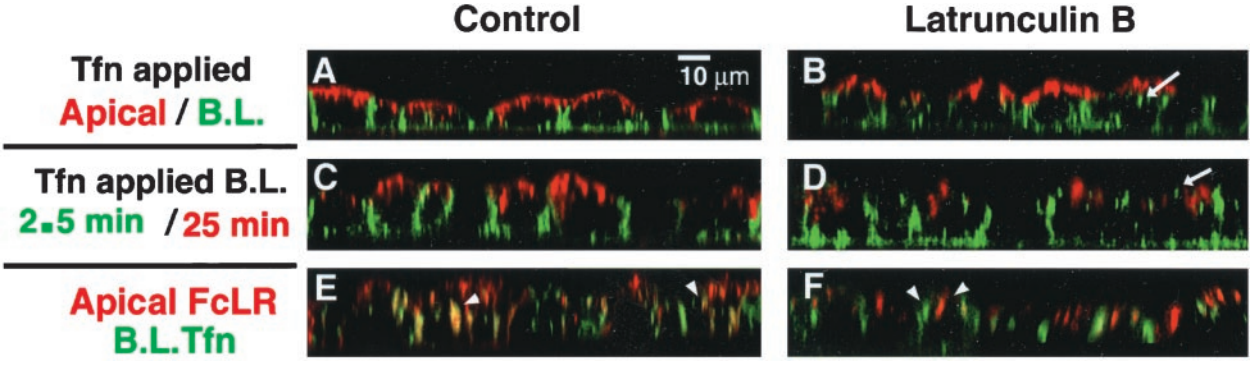

Figure 8. Effects of Lat B on endosomal compartments. Top row, AEE and BEE were selectively labeled with 2-min pulses of basolaterally bound Alexa-488-Tfn and apically bound TR-Tfn. After internalization, surface bound material was stripped with acid wash. Untreated cells (A) and Lat B-treated cells (B), aberrant placement of some early endosomes into more apical and perinuclear regions indicated by arrow in B and D. Middle row, BEE and RE remain distinct after Lat B treatment. Basolaterally bound Alexa-488-Tfn internalized for 2 min (BEE) and basolaterally bound TR-Tfn internalized for 30 min (RE). Untreated cells (C) Lat B-treated cells (D). Bottom row, RE targeting is altered by Lat B. Cells expressing FcLR(5-22) (red, apical) and human TfnR (green, basolateral) were labeled to equilibration then chased for 5 min, and the surface acid stripped to remove surface label. This resulted in preferential labeling of the RE from both sides where labels colocalized (E, arrowheads) and lesser labeling of the early endosomes. Lat B treatment did not affect traffic into RE (as in D) but apical and basolaterally applied labels no longer consistently converged in the same RE (F, arrowheads).

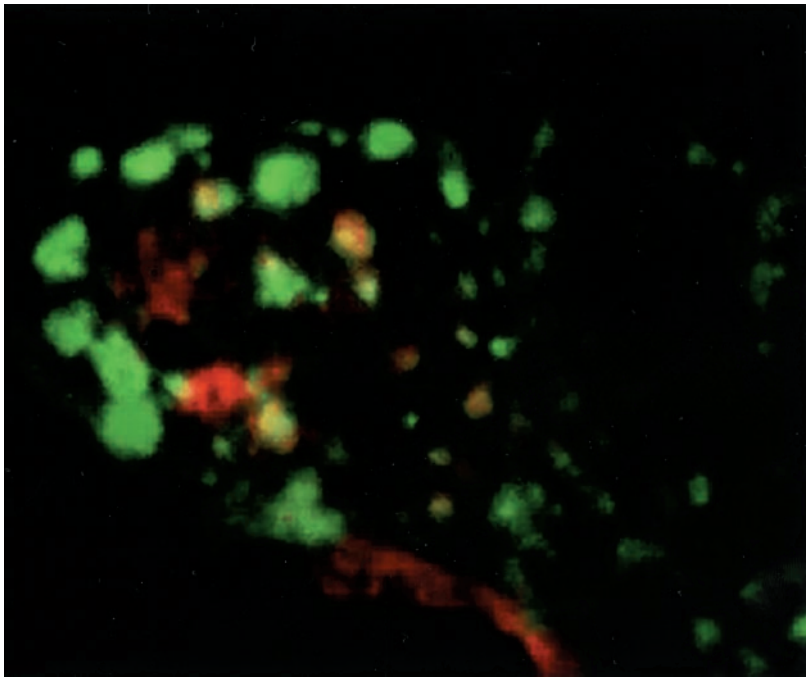

Figure 9. Three-dimensional reconstruction of endosome compartments in MDCK cells (supplemental material). MDCK cells were apically labeled to equilibrium with a Texas Red-labeled antibody to the apical FcLR construct (red). They were labeled basolaterally with a 30-min pulse of Alexa-488-Tfn (green). The cells were chilled, the plasma membrane stripped with low pH to remove surface-bound Tfn and antibody, and then fixed. Green BEE and RE are filled with internalized Tfn. Red endosomes are AEE. Yellow endosomes are RE that contain material endocytosed from apical and basolateral surfaces. The reconstruction may be viewed as a QuickTime video included as supplemental material.

Leung *et al*., 2000; Taunton *et al*., 2000). Our initial observations of Lat B-treated cells indicated a rapid and striking loss of plasma membrane polarity. Although we assumed at first this would reflect a loss of tight junction activity, a rather different mechanism emerged. The basolateral distribution of an LDLR mutant was disrupted, whereas that of an endocytosis-defective LDLR mutant was not affected by Lat B. Demonstrating that Lat B-induced depolarization exhibited an absolute requirement for internalization. Thus, Lat B acted at a step after endocytosis, presumably recycling.

Actin Depolymerization Depolarizes Endosomal Sorting

Lat B profoundly disrupted polarized recycling of TfnR. Sorting of Tfn internalized from the basolateral surface was literally randomized, an effect that was similar in form but far greater in magnitude to that recently observed by Durrbach *et al*. (2000) (using latrunculin A in Caco-2 cells). The reason for this quantitative difference is itself important. In the previous study, Tfn was preloaded for 30 min at 37°C, conditions which would place the majority of the Tfn in the RE population (Sheff *et al*., 1999). Thus, any actin-dependent events that occur at the level of early endosomes would not have been readily detected. By binding Tfn to the basolateral surface on ice and then following the recycling of the Tfn into the media, we were able to monitor changes in sorting in both early endosomes and RE. Indeed, our kinetic analysis strongly suggested that Lat B acted predominantly to cause missorting in basolateral early endosomes.

Lat B treatment had a much smaller effect on the sorting of Tfn internalized from the apical surface, consistent with a primary effect on the BEE. Moreover, if the defect were at the plasma membrane or the tight junction then both apically and basolaterally bound transferrins would be equally affected.

Other studies with cytochalasin D have detected an asymmetric effect on apical but not basolateral membrane traffic of polymeric Ig receptor, folate, and ricin in MDCK cells (Gottlieb *et al*., 1993; Jackman *et al*., 1994; Maples *et al*., 1997). The difference may either be due to the ability of Lat B to depolymerize actin filaments to a greater extent that cytochalasin D or due to differences in internalization mechanisms of the apical plasma membrane protein studied (Maples *et al*., 1997; Durrbach *et al*., 2000).

Functional Pathways of Endocytic Traffic

Our quantitative analysis of the data indicated that the majority of apically internalized Tfn cycled directly from the AEE back to the apical surface. In this respect, the AEE is functionally analogous to the BEE providing a rapid recycling pathway from the early endosome back to the plasma membrane of origin. How then is plasma membrane polarity maintained? Twenty percent of the apically bound Tfn was transcytosed to the basolateral surface, whereas only 5% of basolaterally bound Tfn reached the apical surface. Kinetic modeling suggests that differential sorting to the basolateral side occurs in the RE. Even although only a percentage of membrane traffic passes through the RE, multiple rounds of endocytosis will effectively polarize TfnR to the basolateral surface. Taken together with our previous results demonstrating sorting of transcytotic polymeric IgA receptor from basolateral TfnR in the RE, these results suggest that the RE is a key sorting organelle selectively sorting basolateral from apical traffic over multiple rounds of endocytosis.

Kinetic modeling allowed some insight into the effects of Lat B on endocytic pathways. Surprisingly, merely changing

the magnitude of flux along pathways described in untreated cells (plasma membrane to BEE, BEE to plasma membrane or RE, and RE to plasma membrane) did not account for the effects of Lat B, suggesting that Lat B treatment created a new aberrant pathway. Adding a pathway (k_6) connecting the BEE to the apical plasma membrane (not normally active in control cells) derived a new model with a statistically significant better fit to the data (Figure 7). Traffic along this pathway would effectively depolarize the plasma membrane protein distribution. Conceivably, then, it is in BEEs that the primary effect of Lat B on basolateral TfnR recycling is manifested. Most, but not all of the observed randomization of TfnR recycling could be explained by effects on BEE. The remaining randomization of basolateral traffic, as well as the lesser randomization of apically internalized Tfn could be accounted for by halving the traffic of basolateral receptors from the RE to the basolateral surface rather than increased delivery to the apical surface. The result is that the RE would send roughly equal fluxes of TfnR to the basolateral and apical surfaces respectively (k = 0.021 vs. 0.028) and thus effectively inactivate sorting in the RE. This effect would also explain the lesser degree of missorting observed in cells preloaded with Tfn (Durrbach *et al.*, 1996).

Surprisingly, Lat B interfered with colocalization of apical and basolateral markers in the same RE, although flux through the two RE subsets was the same, suggesting that the convergence of apical and basolateral traffic in a single RE is to some extent guided by actin. Correct sorting in the RE also appears to be actin dependent, suggesting that convergence of apical and basolateral proteins into the RE is required for proper sorting and targeting from the RE.

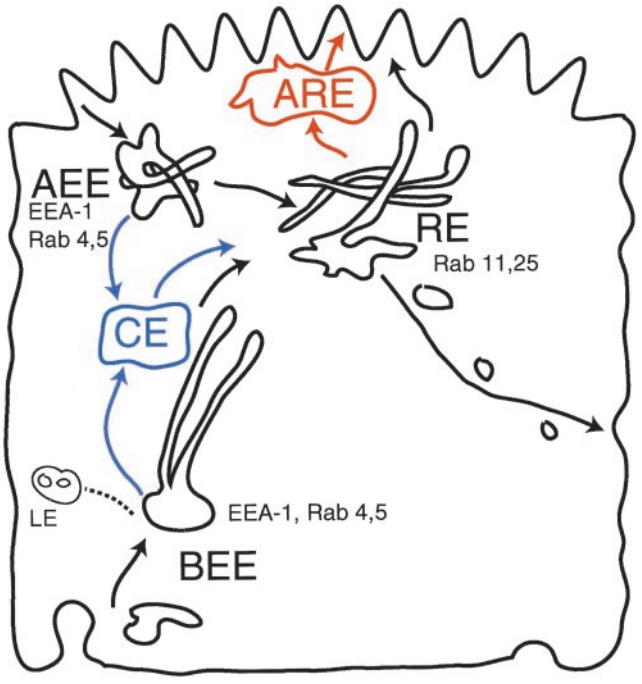

Figure 10. Comparison of endocytic recycling models. The two-compartment model of endocytic recycling pathways used here is illustrated in black. BEEs are portrayed tubulovesicular structures whose tubules extend medially. An additional proposed compartment, the medial common endosome (CE) between the BEE or AEE and the RE is shown with its associated pathways in blue. Another alternative additional compartment, the apical recycling endosome (ARE), between the RE and the apical surface, is shown in red.

Apical and Basolateral Pathways Contain Distinct Early Endosomes

The differential effect on apical versus basolaterally endocytosed Tfn implied that Tfn internalized from each surface passed through distinct compartments. Separate apical and basolateral early endosomes have been proposed based on internalization of fluid phase markers as well as apical and basolateral membrane receptors (Parton *et al.*, 1989; Bomsel *et al.*, 1990). Our system provided the opportunity to test targeting of apically and basolaterally internalized receptors by using the same ligand from each surface. At the level of confocal microscopy, Tfn internalized from the apical and basolateral domains were directed to largely separate populations of apical and basolateral early endosomes. Furthermore, even when the entire apical recycling pathway was equilibrated with the apically restricted FcLR(5-22) chimera, allowing time for diffusion into all early endosomal compartments, none of the chimera colocalized with basolaterally internalized Tfn in BEE. This is consistent with AEE and BEE being distinct structures, but inconsistent with models suggesting a single early endosome population serving both plasma membrane domains (Odorizzi *et al.*, 1996). Even when the BEE was displaced apically by Lat B, it remained functionally distinct from AEE receiving Tfn only from the basolateral surface (Figure 8B).

Kinetic Models of Apical and Basolateral Convergence and Other Kinetic Models

The kinetic model developed herein required a minimum of three compartments to fit the kinetic recycling data (Figure 10, compartments in black). Although the identity of the convergence site(s) between the basolateral and apical endocytic pathways remains uncertain, current concepts would appear to favor this occurring at the level of a recycling endosome population in the apical cytoplasm (Hughson and Hopkins, 1990; Apodaca *et al.*, 1994; Brown *et al.*, 2000; Leung *et al.*, 2000).

It has been suggested that apical and basolateral pathways may converge in a common or medial endosome between early endosomes and RE (Figure 10, blue) (Brown *et al.*, 2000). This model is based on colocalization of basolaterally applied Tfn and apically bound IgA in supranuclear tubular endosomes before sorting of IgA from Tfn. We compared this model with our base model by using data combined from experiments involving apically and basolaterally applied Tfn in control and Lat B-treated cells, as well as previous data from basolaterally applied IgA (Sheff *et al.*, 1999). Inclusion of the additional compartment did not improve the fit of the model to the kinetic data (SS base model = 246, SS common endosome model = 261; $F = -0.3$, $p > 1$). Thus, a common endosome cannot be ruled out on the basis of kinetic data, but neither is it required. Conceivably, this

common endosome may in fact represent the tubular elements of the BEE. In favor of this possibility are the facts that common endosomes share cargo composition with the early endosomes, and that they are largely continuous with fluid-filled vesicular elements of the BEE (Brown *et al*., 2000).

Alternatively, an apical recycling endosome (ARE or SAC) may be interposed between the RE and the apical surface (Figure 10, red) (Ihrke *et al*., 1993; Leung *et al*., 2000; Wang *et al*., 2000). This suggestion was based on observations of transcytotic and apically applied IgA entering a rab11-positive compartment depleted of basolaterally internalized Tfn. Adding an ARE to our model failed to statistically improve the fit of the model to kinetic data (SS base model = 246, SS ARE model = 261; $F = -4.4$, $p > 1$). Moreover, from the data of Brown *et al.* (2000), it is clear that Tfn was not completely excluded from the ARE, but rather exhibited a 5:1 enrichment of transcytotic IgA relative to Tfn. Such an enrichment is predicted to occur in the RE in our model as a result of selective basolateral sorting of Tfn rather than exclusion from the RE (Sheff *et al*., 1999). Furthermore, Rab11 and Tfn receptors were found to colocalize by immunoelectron microscopy and Western blot with RE fractions isolated by density gradient centrifugation (Sheff *et al*., 1999). Thus, it is possible that the subapical, rab11-positive recycling compartment is equivalent to the RE (Sheff *et al*., 1999).

Although kinetic models can never conclusively demonstrate a particular pathway or mechanism, they can be used to rule out those which do not fit the data. Different models were consistent with the kinetic data, but the predicted sites of action of Lat B were essentially the same in all models tested. BEE, AEE, and RE have been identified morphologically as well as biochemically isolated and functionally characterized (Gruenberg *et al*., 1989; Sheff *et al*., 1999). Moreover, they are minimally required kinetically for a mathematical model to fit to recycling data. Although it is entirely possible that additional compartments exist in the apical cytoplasm of MDCK cells (and certainly in other epithelial cell types), at present they have been characterized mostly by the presence or absence of itinerant cargo by using only relatively low-resolution imaging techniques. Thus, transport intermediates may be mistakenly identified as distinct compartments. Until cell fractionation data, functional characterization, and immunocytochemical evidence clearly defines the existence of these structures as compartments, we find it simple to view the endocytic organelles of MDCK cells as close homologs of the EE (apical or basolateral) and RE found in "nonpolarized" cells.

CONCLUSION

Although our efforts have not elucidated the molecular mechanism involved, they have defined the likely sites at which actin is important. Conceivably, one can imagine that actin association is required to allow BEE to generate vesicles targeted to the basolateral surface. Alternatively, or in addition, actin may be required simply to ensure the localization of BEE in the basolateral region of the cell, limiting the chances for docking and fusion with the incorrect apical surface. Actin also appears to play a role in polarized sorting in the RE. It remains to be seen how this association with actin is regulated differentially along the endocytic pathway.

ACKNOWLEDGMENTS

This work was supported by grants to I.M. from the National Institutes of Health and to D.S. from the Patrick and Catherine Weldon Donaghue Medical Research Foundation. I.M. is an Affiliate Member of the Ludwig Institute for Cancer Research.

REFERENCES

Apodaca, G. (2001). Endocytic traffic in polarized epithelial cells: role of the actin and microtubule cytoskeleton. Traffic *2*, 149–159.

Apodaca, G., Katz, L.A., and Mostov, K.E. (1994). Receptor-mediatedtranscytosis of IgA in MDCK cells is via apical recycling endosomes. J. Cell Biol. *125*, 67–86.

Balda, M.S., and Matter, K. (1998). Tight junctions. J. Cell Sci. *111*, 541–547.

Bomsel, M., Parton, R., Kuznetsov, S.A., Schroer, T.A., and Gruenberg, J. (1990). Microtubule- and motor-dependent fusion in vitro between apical and basolateral endocytic vesicles from MDCK cells. Cell *62*, 719–731.

Brown, P.S., Wang, E., Areoti, B., Chapin, S.J., Mostov, K.E., and Dunn, K.E. (2000). Definition of distinct compartments in polarized Madin-Darby canine kidney (MDCK) cells for membrane-volume sorting, polarized sorting and apical recycling. Traffic *1*, 124–140.

Depina, A.S., and Langford, G.M. (1999). Vesicle transport: the role of actin filaments and myosin motors. Microsc. Res. Tech. *47*, 93–106.

Drubin, D.G., and Nelson, W.J. (1996). Origins of cell polarity. Cell *84*, 335–344.

Durrbach, A., Louvard, D., and Coudrier, E. (1996). Actin filaments facilitate two steps of endocytosis. J. Cell Sci. *109*, 457–465.

Durrbach, A., Raposo, G., Tenza, D., Louvard, D., and Coudrier, E. (2000). Truncated rush border myosin I affects membrane traffic in polarized epithelial cells. Traffic *1*, 411–424.

Ellis, S., and Mellor, H. (2000). Regulation of endocytic traffic by rho family GTPases. Trends Cell Biol. *10*, 85–88.

Fath, K.R., Trimbur, G.M., and Burgess, D.R. (1997). Molecular motors and a spectrin matrix associate with Golgi membranes in vitro. J. Cell Biol. *139*, 1169–1181.

Fujimoto, M.L., Roth, R., Heuser, J.E., and Schmid, S.L. (2000). Actin assembly plays a variable, but not obligatory role in receptor-mediated endocytosis in mammalian cells. Traffic *1*, 161–171.

Gaidarov, I., Santini, F., Warren, R.A., and Keen, J.H. (1999). Spatial control of coated-pit dynamics in living cells. Nat. Cell Biol. *1*, 1–7.

Gottlieb, T.A., Ivanov, I.E., Adesnik, M., and Sabatini, D.D. (1993). Actin microfilaments play a critical role in endocytosis at the apical but not the basolateral surface of polarized epithelial cells. J. Cell Biol. *120*, 695–710.

Gronewold, T.M., Sasse, F., Lunsdorf, H., and Reichenbach, H. (1999). Effects of rhizopodin and latrunculin b on the morphology and on the actin cytoskeleton of mammalian cells. Cell Tissue Res *295*, 121–9.

Gruenberg, J., Griffiths, G., and Howell, K.E. (1989). Characterization of the early endosome and putative endocytic carrier vesicles in vivo and with an assay of vesicle fusion in vitro. J. Cell Biol. *108*, 1301–1316.

Huber, L.A., Fialka, I., Paiha, K., Hunziker, W., Sacks, D.B., Bahler, M., Way, M., Gagescu, R., and Gruenberg, J. (2000). Both calmodulin and the unconventional myosin myr4 regulate membrane trafficking along the recycling pathway of MDCK cells. Traffic *1*, 494–503.

Hughson, E.J., and Hopkins, C.R. (1990). Endocytic pathways in polarized Caco-2 cells: identification of an endosomal compartment accessible from both apical and basolateral surfaces. J. Cell Biol. *110*, 337–348.

Ihrke, G., Neufeld, E.B., Meads, T., Shanks, M.R., Cassio, D., Laurent, M., Schroer, T.A., Pagano, R.E., and Hubbard, A.L. (1993). Wif-b cells: an in vitro model for studies of hepatocyte polarity. J. Cell Biol. *123*, 1761–75.

Jackman, M.R., Shurety, W., Ellis, J.A., and Luzio, J.P. (1994). Inhibition of apical but not basolateral endocytosis of ricin and folate in caco-2 cells by cytochalasin d. J. Cell Sci. *107*, 2547–2556.

Kessels, M.M., Engqvist-Goldstein, A.E.Y., Drubin, D.G., and Qualmannn, B. (2001). Mammalian abp1, a signal-responsive f-actin-binding protein, links the actin cytoskeleton to endocytosis via the GTPase dynamin. J. Cell Biol. *153*, 1–16.

Kroschewski, R., Hall, A., and Mellman, I. (1999). Cdc42 controls secretory and endocytic transport to the basolateral plasma membrane of MDCK cells. Nat. Cell Biol. *1*, 8–13.

Lamaze, C., Fujomoto, L.M., Yin, H.L., and Schmid, S.L. (1997). The actin cytoskeleton in required for receptor-mediated endocytosis in mammalian cells. J. Biol. Chem. *272*, 20332–20335.

Leung, S.M., Ruiz, W.G., and Apodaca, G. (2000). Sorting of membrane and fluid at the apical pole of polarized Madin-Darby canine kidney cells. Mol. Biol. Cell *11*, 2131–2150.

Lipsky, N.G., and Pagano, R.E. (1983). Sphingolipid metabolism in cultured fibroblasts: microscopic and biochemical studies employing a fluorescent ceramide analogue. Proc. Natl. Acad. Sci. USA *80*, 2608–2612.

Maples, C.J., Ruiz, W.G., and Apodaca, G. (1997). Both microtubules and actin filaments are required for efficient postendocytic traffic of the polymeric immunoglobulin receptor in polarized Madin-Darby canine kidney cells. J. Biol. Chem. *272*, 6741–6751.

Matter, K., Whitney, J.A., Miller, E., and Mellman, I. (1993). Common signals control LDL receptor sorting in endosomes and the Golgi of MDCK cells. Cell *74*, 1053–1064.

Mellman, I. (1996). Endocytosis and molecular sorting. Annu. Rev. Cell Dev. Biol. *12*, 575–625.

Merrifield, C.J., Moss, S.E., Ballestrem, C., Imhof, B.A., Giese, G., Wunderlich, I., and Almers, W. (1999). Endocytic vesicles move at the tips of actin tails in cultured mast cells. Nat. Cell Biol. *1*, 72–74.

Musch, A., Cohen, D., Kreitzer, G., and Rodriguez-Boulan, E. (2001). Cdc42 regulates the exit of apical and basolateral proteins from the trans-Golgi network. EMBO J. *20*, 2171–2179.

Odorizzi, G., Pearse, A., Domingo, D., Trowbridge, I.S., and Hopkins, C.R. (1996). Apical and basolateral endosomes of MDCK cells are interconnected and contain a polarized sorting mechanism. J. Cell Biol. *135*, 139–152.

Parton, R.G., Prydz, K., Bomsel, M., Simons, K., and Griffiths, G. (1989). Meeting of the apical and basolateral endocytic pathways of the Madin-Darby canine kidney cell in late endosomes. J. Cell Biol. *109*, 3259–3272.

Raposo, G., Cordonnier, M.N., Tenza, D., Menichi, B., Durrbach, A., Louvard, D., and Coudrier, E. (1999). Association of myosin I alpha with endosomes and lysosomes in mammalian cells. Mol. Biol. Cell *10*, 1477–1494.

Rodriguez-Boulan, E., and Powell, S.K. (1992). Polarity of epithelial and neuronal cells. Annu. Rev. Cell. Biol. *8*, 395–427.

Sheff, D.R., Daro, E.A., Hull, M., and Mellman, I. (1999). The receptor recycling pathway contains two distinct populations of early endosomes with different sorting functions. J. Cell Biol. *145*, 123–139.

Sonnichsen, B., De Renzis, S., Nielsen, E., Rietdorf, J., and Zerial, M. (2000). Distinct membrane domains on endosomes in the recycling pathway visualized by multicolor imaging of rab4, rab5, and rab11 [in process citation]. J. Cell Biol. *149*, 901–914.

Spector, I., Shochet, N.R., Kashman, Y., and Groweiss, A. (1983). Latrunculins: novel marine toxins that disrupt microfilament organization in cultured cells. Science *219*, 493–5.

Stow, J.L., Fath, K.R., and Burgess, D.R. (1998). Budding roles for myosin ii on the Golgi. Trends Cell Biol. *8*, 138–141.

Taunton, J., Rowning, B.A., Coughlin, M.L., Wu, M., Moon, R.T., Mitchison, T.J., and Larabell, C.A. (2000). Actin-dependent propulsion of endosomes and lysosomes by recruitment of n-wasp() [in process citation]. J. Cell Biol. *148*, 519–530.

Van Meer, G., Stelzer, E.H., Wijnaendts-Van-Resandt, R.W., and Simons, K. (1987). Sorting of sphingolipids in epithelial (Madin-Darby canine kidney) cells. J. Cell Biol. *105*, 1623–1635.

Wakatsuki, T., Schwab, B., Thompson, N.C., and Elson, E.L. (2001). Effects of cytochalasin D and latrunculin B on mechanical properties of cells. J. Cell Sci. *114*, 1025–1036.

Wang, E., Brown, P.S., Aroeti, B., Chapin, S.J., Mostov, K.E., and Dunn, K.W. (2000). Apical and basolateral endocytic pathways of MDCK cells meet in acidic common endosomes distinct from a nearly-neutral apical recycling endosome. Traffic *1*, 480–493.

Winckler, B., Forscher, P., and Mellman, I. (1999). A diffusion barrier maintains distribution of membrane proteins in polarized neurons [see comments]. Nature *397*, 698–701.

Zahraoui, A., Louvard, D., and Galli, T. (2000). Tight junction, a platform for trafficking and signaling protein complexes. J. Cell Biol. *151*, F31–F36.